

Research Article: New Research | Neuronal Excitability

### Synaptic plasticity at inhibitory synapses in the ventral tegmental area depends upon stimulation site

https://doi.org/10.1523/ENEURO.0137-19.2019

Cite as: eNeuro 2019; 10.1523/ENEURO.0137-19.2019

Received: 10 April 2019 Revised: 16 September 2019 Accepted: 4 October 2019

This Early Release article has been peer-reviewed and accepted, but has not been through the composition and copyediting processes. The final version may differ slightly in style or formatting and will contain links to any extended data.

Alerts: Sign up at www.eneuro.org/alerts to receive customized email alerts when the fully formatted version of this article is published.

### Copyright © 2019 St. Laurent and Kauer

This is an open-access article distributed under the terms of the Creative Commons Attribution 4.0 International license, which permits unrestricted use, distribution and reproduction in any medium provided that the original work is properly attributed.

1			
2			
3 4	Synaptic plasticity at inhibitory synapses in the ventral tegmental area depends upon stimulation site		
5			
6			
7	Robyn St. Laurent <sup>1,2</sup> and Julie Kauer <sup>1</sup>		
8	<sup>1</sup> Department of Psychiatry & Behavioral Sciences, Stanford University School of Medicine,		
9	Stanford, CA 94305		
10 11	<sup>2</sup> Gladstone Institutes, 1650 Owens Street, San Francisco, CA 94158		
12			
13			
14 15 16 17 18 19 20	Correspondence should be addressed to: Julie A. Kauer, Ph.D. Department of Psychiatry & Behavioral Sciences Stanford University School of Medicine, MSLS P-104 Stanford, CA 94305 jkauer@stanford.edu		
21 22 23	Abbreviated Title (50 character maximum): Heterogenous Inhibitory Synaptic Plasticity in VTA		
24	Acknowledgements		

#### Acknowledgements:

- The authors wish to thank Ayumi Tsuda for technical help, and to acknowledge funding from the
- NIH: NIDA 011289 (JAK), T32 MH20068 (RS) and NIDA F31DA045419 (RS).

### 28 ABSTRACT

29 Drug exposure induces cell and synaptic plasticity within the brain reward pathway that could be 30 a catalyst for progression to addiction. Several cellular adaptations have been described in the ventral tegmental area (VTA), a central component of the reward pathway that is the major 31 source of dopamine release. For example, administration of morphine induces long-term 32 potentiation (LTP) of excitatory synapses on VTA dopamine cells and blocks LTP at inhibitory 33 34 synapses. Drug-induced synaptic changes have a common endpoint of increasing dopamine 35 cell firing and dopamine release. However, gaining a complete picture of synaptic plasticity in the VTA is hindered by its complex circuitry of efferents and afferents. Most studies of synaptic 36 plasticity in the VTA activated a mixed population of afferents, potentially yielding an incomplete 37 and perhaps misleading view of how drugs of abuse modify VTA synapses. Here, we use 38 39 midbrain slices from mice and find that electrical stimulation in two different regions induces different forms of plasticity, including two new forms of LTP at inhibitory synapses. High 40 frequency stimulation induces LTP independently of NMDA receptor activation, and surprisingly, 41 42 some inhibitory inputs to the VTA also undergo NMDAR-independent LTP after a low frequency stimulation (LFS) pairing protocol. 43

44

### 45 SIGNIFICANCE STATEMENT

Synaptic plasticity of inhibitory inputs onto dopamine cells in the ventral tegmental area has a major influence on the circuits implicated in addictive behaviors. The location of electrical stimulation in an acute midbrain slice dictated the response of inhibitory inputs to plasticity induction protocols. We describe a new form of synaptic strengthening that occurs at an opioidsensitive input to the ventral tegmental area. 51

### 52 **INTRODUCTION**

53 The ventral tegmental area (VTA) contains dopaminergic cells that receive inhibitory innervation from γ-aminobutyric acid (GABA)-ergic cell bodies originating within the VTA and from many 54 55 other brain regions (Watabe-Uchida et al., 2012, Beier et al., 2015). Despite a wealth of 56 anatomical and behavioral studies investigating the diversity of VTA afferents, plasticity at inhibitory synapses was historically described without identification of the presynaptic partner 57 (Melis et al., 2002, Liu et al., 2005, Nugent et al., 2009, Nugent et al., 2007, Niehaus et al., 58 2010, Dacher and Nugent, 2011, Padgett et al., 2012, Kodangattil et al., 2013, Graziane et al., 59 2013, Polter et al., 2014). For example, nitric-oxide dependent long-term potentiation (LTPGABA) 60 61 can be triggered using electrical stimulation within the VTA (Nugent et al., 2007), however, when specific afferents were isolated using optogenetics, induction of LTPGABA was found to 62 depend upon the presynaptic partner (Simmons et al., 2017, Polter et al., 2018). Specifically, 63 64 LTP<sub>GABA</sub> is expressed at nucleus accumbens and VTA GABA<sub>A</sub> synapses, but not rostromedial 65 tegmental nucleus (RMTg)-originating GABA<sub>A</sub> synapses. These observations demonstrate that 66 all GABAergic synapses cannot be assumed to share a common plasticity mechanism. The idea 67 that plasticity is segregated to specific populations is not a new one, and in fact many reports 68 segregate experiments by postsynaptic cell identity. For example, long-term depression (LTD) induced by low frequency afferent stimulation is only expressed in putative dopamine cells in the 69 70 VTA that express large H currents ( $I_h$ ) (Dacher and Nugent, 2011). With local electrical 71 stimulation in acute slices, it is possible to isolate synapses of one neurotransmitter type pharmacologically, but the identity of the presynaptic source is not always as easy to manipulate 72 or determine. Although the location of the postsynaptic VTA cell (e.g. medial vs. lateral VTA) 73 74 can sometimes predict output site, inputs from over 20 brain regions contact dopamine cells in

all VTA subregions (Beier et al., 2015). It is possible that other plasticity mechanisms have yet to be uncovered because their expression is limited to a subset of inputs, and therefore not apparent with global activation of all inputs. Here we use different electrical stimulation sites, and report two ways of inducing LTP at inhibitory synapses in the VTA with a mechanism(s) that is non-overlapping with that of  $LTP_{GABA}$  or other known forms of LTP at inhibitory synapses in the VTA.

81

### 82 METHODS

### 83 1. Animals:

84 All procedures were carried out in accordance with the guidelines of the National Institutes of Health for animal care and use and were approved by the [Author University] Institutional 85 Animal Care and Use Committee. This study used VGAT::IRES-Cre (RRID:IMSR\_JAX:028862, 86 strain code: B6J.129S6(FVB)-Slc32a1<sup>tm2(cre)Lowl</sup>), DAT::IRES-Cre (RRID:IMSR\_JAX:006660, 87 strain code: B6.SJL-Slc6a3<sup>tm1.1(cre)Bkmn/J</sup>) (Zhuang et al., 2005), Ai14 Cre-reporter mice 88 B6;129S6-Gt(ROSA)26Sor<sup>tm14(CAG-tdTomato)Hze/J</sup>), (RRID:IMSR JAX:007908, code: 89 strain 90 VGAT-ChR2(H134R)-EYFP (RRID:IMSR JAX:014548, strain code: B6.Ca-Ta(Slc32a1-COP4\*H134R/EYFP)8Gfng/J; (Zhao et al., 2011), and C57BL/6 (RRID:IMSR\_JAX:000664) 91 male and female mice bred in-house. Mice were maintained on a 12-h light/dark cycle and 92 provided food and water ad libitum. 93

94

### 95 2. Preparation of brain slices

Horizontal brain slices (220 µm) were prepared from deeply anesthetized mice. Briefly,
anesthetized mice were perfused with ice-cold oxygenated artificial cerebrospinal fluid (ACSF)

98 (in mM): 126 NaCl, 21.4 NaHCO<sub>3</sub>, 2.5 KCl, 1.2 NaH<sub>2</sub>PO<sub>4</sub>, 2.4 CaCl<sub>2</sub>, 1.0 MgSO<sub>4</sub>, 11.1 glucose, 5 sodium ascorbate. Following perfusion, the brain was rapidly dissected and horizontal slices 99 (220 µm) were prepared using a vibratome. Slices recovered for 1 h at 34°C in oxygenated 100 HEPES holding solution (in mM): 86 NaCl, 2.5 KCl, 1.2 NaH<sub>2</sub>PO<sub>4</sub>, 35 NaHCO<sub>3</sub>, 20 HEPES, 25 101 glucose, 5 sodium ascorbate, 2 thiourea, 3 sodium pyruvate, 1 MgSO<sub>4</sub>.7H<sub>2</sub>O, 2 CaCl<sub>2</sub>.2H<sub>2</sub>O 102 103 (Ting et al., 2014), and then were held in the same HEPES solution at room temperature until use. Slices were then transferred to a recording chamber where they were submerged in ACSF 104 105 without sodium ascorbate.

106

### 107 3. Electrophysiology

108 Electrophysiological experiments were performed in horizontal midbrain slices containing the VTA that were continuously perfused with ACSF containing 10 µM 6,7-dinitroquinoxaline- 2,3-109 dione (DNQX) and 1 µM strychnine, AMPA and glycine receptor antagonists, respectively. 110 111 Except where noted, recordings also included the NMDA receptor antagonist d-APV (50 or 100 μM). Whole-cell recordings were performed from neurons in the lateral VTA with KCl pipette 112 solution and voltage-clamped at -70mV. Patch pipettes were filled with (in mM): 125 KCl, 2.8 113 114 NaCl, 2 MgCl<sub>2</sub>, 2 ATP-Na<sup>+</sup>, 0.3 GTP-Na<sup>+</sup>, 0.6 EGTA, and 10 HEPES. In some experiments EGTA was increased to 15 mM, or GDP-β-S (1 mM) was included in the pipette solution as 115 116 noted. The presence of a large hyperpolarization-activated inward current was used to select 117 postsynaptic cells for recording, although we are aware that this metric can allow inclusion of a 118 subset of non-dopamine neurons. If the steady-state h-current was greater than 25 pA during a 119 step from -50 mV to -100 mV, the cell was included in analyses. In a subset of recordings, 120 dopamine cells were also identified via fluorescence imaging using a DAT::IRES-cre x 121 TdTomato reporter line. All experiments were performed at 30°C, maintained by an automatic

temperature controller. The series resistance was monitored continuously during the experimentand cells were discarded for deviations >15%.

124

#### 125 4. Stimulation protocols

126 For electrical stimulation, a bipolar stainless steel stimulating electrode was placed caudal to the 127 VTA approximately 500 µm from the recorded cell; for rostral placement the stimulating 128 electrode was placed within the VTA at 200-500 μm from the recorded cell (Figure 1A). Inhibitory postsynaptic currents (IPSCs) were evoked at 0.1 Hz using 100µs current pulses. We 129 used input-output curves to identify the stimulation intensity used for plasticity experiments for 130 131 both rostral and caudal afferents, and the baseline amplitude was at 50% of this generated 132 curve. No correlation was observed between stimulation intensity and LTP magnitude. This stimulation protocol did not produce action potentials escaping voltage-clamp, but in the rate 133 cases that cells began spiking later in the recording, they were excluded from analysis. 134 Channelrhodopsin-induced synaptic currents were evoked at 0.033 Hz using 0.1-5 ms light 135 136 pulses from a white LED (Mightex) controlled by driver (ThorLabs) and reflected through a 40x 137 water immersion lens. When feasible, IPSCs were shown to be GABAA receptor-mediated by 138 bath application of 10 µM bicuculline at the end of recordings. For all stimulus frequencies, 139 intensity remained constant throughout the experiment.

140

### 141 5. Statistical analysis

Results are expressed as mean +/- standard error of the mean (S.E.M.). Significance was determined using a two-tailed paired Student's t-test or one-way analysis of variance (ANOVA) with significance level of p < 0.05. LTP values are reported as averaged IPSC amplitudes for 10 min just before LTP induction compared with averaged IPSC amplitudes during the 10-min

period from 10–20 min after manipulation. Paired-pulse ratios (50 ms interstimulus interval) and coefficient of variation were measured over 10 min epochs of 10-30 IPSCs each. The paired pulse ratio was calculated using the average value for all IPSC2 amplitudes divided by the average value for the corresponding IPSC1 amplitudes and reported as the mean paired pulse ratio for that epoch. Coefficient of variance analysis of 1/CV<sup>2</sup> values were determined by dividing the mean amplitude of IPSCs squared recorded over 10 minute epochs by the mean variance of these IPSCs.

153

### 154 6. Materials

6,7-Dinitroquinoxaline-2,3[1H,4H]-dione (DNQX) were obtained from Sigma-Aldrich. D-2-Amino5-phosphonopentanoic acid (APV), bicuculline, [D-Ala<sup>2</sup>, NMe-Phe<sup>4</sup>, Gly-ol<sup>5</sup>]-enkephalin
(DAMGO), forskolin, and naloxone were obtained from Tocris. Strychnine was obtained from
Tocris or Abcam.

159

### 160 RESULTS

### 161 Location of electrical stimulation determines expression of synaptic plasticity

Most reports examining synaptic plasticity in the VTA have used a stimulating electrode placed within the VTA 200-500  $\mu$ M rostral to the recorded cell in a horizontal slice (Figure 1A). This approach has been assumed to randomly sample the synaptic inputs onto cells within the VTA. We hypothesized that stimulating caudal to and outside of the VTA, approximately 500  $\mu$ M from the recorded cell, might bias the inputs differently than with a rostral placement (Figure 1A). We refer to this as "caudal" stimulation. We recorded inhibitory postsynaptic potentials (IPSCs) in putative dopamine cells identified by a large I<sub>h</sub> and compared synaptic properties using either 169 caudal or rostral electrical stimulation. We did not detect any differences between IPSCs evoked by rostral or caudal stimulation in the onset delay, rise slope, or time of peak amplitude of IPSCs 170 (Figure 1B-D; paired t test of rostral vs. caudal onset delay:  $p = 0.82^{a}$ ; rise slope:  $p = 0.74^{b}$ ; time 171 of peak: p = 0.98 °; rostral: n = 15 cells, caudal: n = 18 cells). Opioids depress GABAergic 172 inhibition in the VTA, therefore we compared the opioid-sensitivity of caudal and rostral-173 174 stimulated IPSCs. IPSCs from both stimulating locations were depressed by 1 µM [D-Ala<sup>2</sup>, N-MePhe<sup>4</sup>, Gly-ol]-enkephalin (DAMGO) to the same degree (Figure 1E-F; rostral = -55 ± 8%, 175 n = 6 cells; caudal = -58  $\pm$  9%, n = 13 cells; rostral vs. caudal:  $p = 0.86^{d}$ ). Thus, synaptic 176 properties were similar when stimulating either the rostral or caudal site. 177

178

179 We next used a stimulation protocol known to induce the nitric oxide-dependent LTPGABA: high frequency stimulation (HFS) consisting of two 100 Hz tetani separated by 10 seconds (Nugent 180 et al., 2007). LTP<sub>GABA</sub> is dependent on NMDA receptor (NMDAR) activation that leads to the 181 182 release of nitric oxide and activation of a signaling cascade that increases presynaptic GABA release (Nugent et al., 2007, Nugent et al., 2009). Instead, HFS of the caudally stimulated site 183 resulted in LTP, even with the NMDAR antagonist, APV (100 µM), in the bath solution (Figure 184 2A,B,E; 157  $\pm$  23% of baseline value; paired t test:  $p = 0.018^{\circ}$ , n = 16 cells). Conversely and 185 consistent with prior results, the same tetanus of a rostrally-placed electrode did not potentiate 186 IPSCs in APV ((Nugent et al., 2007); Figure 2C-E;  $90 \pm 11\%$  of baseline value; paired t test: p =187 0.73<sup>f</sup>, n = 6 cells). Potentiation after HFS of the caudally-stimulated electrode was correlated 188 with a decrease in paired pulse ratio for cells that potentiated by at least by 10% (Figure 2F; 189 baseline baseline: 1.1 +/- 0.2, after HFS: 0.9 +/- 0.1), without a change in 1/CV<sup>2</sup> values (Figure 190 2G; baseline: 7.5  $\pm$  2.1, 10-20 min after HFS: 8.1  $\pm$  1.4; paired t test:  $p = 0.048^{9}$  and  $p = 0.70^{h}$ , 191 192 respectively, n = 12 cells). These findings supported our hypothesis that electrode placement

may activate different subsets of afferents and lead to a different outcome when performingprotocols to induce synaptic plasticity.

195

### 196 Low frequency stimulation potentiates caudal-evoked inhibitory inputs

197 Inhibitory synapses can be regulated bidirectionally by different afferent stimulation patterns. In an earlier study, low frequency stimulation (LFS) of afferents by a stimulating electrode placed 198 rostral to the VTA cell being recorded was used to elicit long term depression (LTD). LTD is 199 induced by LFS, 6 minutes of 1 Hz stimulation while voltage clamping the postsynaptic cell at -200 40 mV (LFS-LTD; (Dacher and Nugent, 2011)). LFS-LTD occurs independently of NMDAR 201 202 activation and is partially blocked by a dopamine D2 receptor antagonist (Dacher and Nugent, 2011). Given the surprising result with HFS of a caudally-placed electrode, we asked whether 203 LFS of a caudally-placed stimulating electrode would also induce LTD. Instead, LFS of caudally-204 205 evoked IPSCs triggered LTP both in the absence or presence of APV (LFS-LTPGABA)(Figure 3A-D; 131 ± 10% of baseline value;  $p = 0.026^{\circ}$ , n = 38 cells). PPR was not significantly altered in 206 cells potentiating by at least 10% after LFS (Figure 3E; baseline: 1.0 ± 0.1, 10-20 min after 207 LFS: 0.9 ± 0.1;  $p = 0.058^{j}$ , n = 22 cells) and neither were the normalized 1/CV<sup>2</sup> values (Figure 208 3F; baseline: 5.7 ± 1.1, 10-20 min after LFS: 7.8 ± 1.8; p = 0.09<sup>k</sup>, n = 19 cells). This surprising 209 finding led us to conclude that as with HFS-induced LTP, previous observations of LTD 210 211 following LFS were likely dependent upon activation of a subset of VTA afferents.

212

### 213 LFS of optically-evoked inhibitory inputs in the VTA does not induce plasticity

There are many sources of GABAergic inhibition in the VTA and given that LFS can induce either LTD or LTP, depending on stimulation site, we wondered which form of plasticity was predominant when activating GABAergic synapses more globally. We hypothesized that just a 217 subset of VTA synapses express LFS-LTP<sub>GABA</sub>, so that when using optical stimulation of VGAT+ inputs in a VGAT-ChR2 transgenic mouse line, both forms of plasticity might occur at different 218 synapses on the same dopamine cell. We used a BAC transgenic mouse line, 219 VGAT-ChR2(H134R)-EYFP, to activate multiple GABAergic inputs in the VTA (Zhao et al., 220 221 2011), and used whole field LED illumination of the slice to activate inhibitory inputs. After 222 generating a stable 10 minute baseline of light-evoked IPSCs, we delivered optical LFS while depolarizing the postsynaptic cell to -40 mV. In contrast to what we observed with caudal 223 electrical stimulation, the mean light-evoked IPSC amplitude was unchanged after optical LFS 224 225 (Figure 4A-C; 102  $\pm$  10% of baseline value;  $p = 0.83^{l}$ , n = 7 cells). PPR was not significantly altered after LFS (data not shown; baseline: 0.72 ± 0.07, 10-20 min after LFS: 0.72 ± 0.05, 226  $p = 0.97^{\text{m}}$ , n = 7 cells) and neither were 1/CV<sup>2</sup> values (data not shown; baseline: 20.0 ± 2.4, 10-227 228 20 min after LFS:  $20.2 \pm 3.6$ ,  $p = 0.95^{n}$ , n = 7 cells).

229

### 230 Forskolin potentiation does not occlude LFS-induced LTP

231 Forskolin is known to potentiate many synapses. Forskolin activates adenylyl cyclase which 232 potentiates GABAergic synapses in the VTA (Melis et al., 2002, Nugent et al., 2009) as well as at many excitatory and inhibitory synapses throughout the CNS (Briggs et al., 1988, Greengard 233 et al., 1991, Cameron and Williams, 1993, Chavez-Noriega and Stevens, 1994, Huang and 234 235 Kandel, 1994, Weisskopf et al., 1994, Bonci and Williams, 1996, Salin et al., 1996, Bonci and Williams, 1997, Huang and Kandel, 1998, Castro-Alamancos and Calcagnotto, 1999, Linden 236 and Ahn, 1999, Mellor et al., 2002). Both prior VTA studies using forskolin and stimulating 237 GABAergic VTA afferents used rostral electrical stimulation. We wondered if forskolin would 238 also potentiate inputs evoked with caudal afferent stimulation or whether these synapses would 239 240 prove distinct again. We found that 10 µM forskolin potentiated IPSCs stimulated with a 241 caudally-placed electrode (Figure 5A-C; 183  $\pm$  19% of baseline value;  $p = 0.003^{\circ}$ , n = 14 cells), although PPR was not significantly altered after forskolin (data not shown; baseline:  $0.9 \pm 0.1$ , 10-20 min after LFS:  $0.9 \pm 0.1$ ;  $p = 0.65^{p}$ , n = 13 cells). Forskolin potentiation occludes NMDARdependent LTP<sub>GABA</sub> (Nugent et al., 2009). Therefore, we performed occlusion experiments to ask if forskolin potentiation occludes caudal LFS-induced LTP. However, forskolin-induced potentiation did not occlude further potentiation by LFS (Figure 5D-F; 131 ± 10% of baseline value;  $p = 0.046^{q}$ , n = 10 cells). These data suggest that the mechanism underlying LFSinduced LTP is distinct from that of forskolin potentiation.

249

## LFS-induced LTP does not require postsynaptic GPCR signaling and is not prevented by postsynaptic EGTA

252 Potentiation after LFS was not associated with a significant change in the paired pulse ratio or 253 coefficient of variation (see Figure 3E-F), suggesting that the mechanism may reflect an 254 increased GABAergic sensitivity of the postsynaptic cells. Most forms of LTP are triggered by 255 increases in calcium concentration in the postsynaptic cell, and so we tested whether LFS-LTP requires a rise in postsynaptic calcium. When the concentration of the calcium chelator, EGTA, 256 257 was raised to 15mM in the patch pipette, LFS still resulted in potentiation of caudally-evoked IPSCs (Figure 6A-C; 155 ± 24% of baseline value; n = 8 cells). An alternative postsynaptic 258 mechanism might require activation of receptors on the postsynaptic cell other than GABAA 259 260 receptors. For example, the report of LFS-LTD found that depression was partially dependent upon dopamine D2 receptors (Dacher and Nugent, 2011), which are coupled to the G<sub>i</sub> subtype 261 of G-protein coupled receptors (GPCR). When we included an inhibitor of GPCR activity (1 mM 262 GDP-βS) in the patch pipette to block all postsynaptic GPCR signaling, LFS still potentiated 263 caudally-evoked IPSCs (Figure 6D-F; 135 ± 8% of baseline value; n = 8 cells). The magnitude 264 265 of LTP after LFS was not significantly different for high EGTA or GDP-β-S conditions than experiments with normal KCI internal solution (F(2,27) = 0.77,  $p = 0.48^{r}$ , n = 8 cells high EGTA, 266

n = 8 cells GDP-β-S, n = 14 cells normal KCl). Together our results suggest a mechanism that does not require postsynaptic GPCRs or Ca<sup>2+</sup> influx. Future experiments will be needed to understand this novel form of LTP.

270

271 Statistical Table.

Data Structure	Type of Test	95% confidence interval
<sup>a</sup> normal distribution	two-tailed unpaired t-test	-0.79 to 0.98
<sup>b</sup> normal distribution	two-tailed unpaired t-test	-85.83 to 119.6
<sup>c</sup> normal distribution	two-tailed unpaired t-test	-0.99 to 1.01
<sup>d</sup> normal distribution	two-tailed unpaired t-test	-27.21 to 32.06
<sup>e</sup> normal distribution	two-tailed paired t-test	18.20 to 162.8
<sup>f</sup> normal distribution	two-tailed paired t-test	-78.82 to 59.01
<sup>g</sup> normal distribution	two-tailed paired t-test	-0.43 to -0.002
<sup>h</sup> normal distribution	two-tailed paired t-test	-2.47 to 3.56
<sup>i</sup> normal distribution	two-tailed paired t-test	5.89 to 85.91
<sup>j</sup> normal distribution	two-tailed paired t-test	-0.17 to 0.0029
<sup>k</sup> normal distribution	two-tailed paired t-test	-0.38 to 4.43
<sup>1</sup> normal distribution	two-tailed paired t-test	-87.36 to 104.7
<sup>m</sup> normal distribution	two-tailed paired t-test	-0.15 to 0.15
<sup>n</sup> normal distribution	two-tailed paired t-test	-9.54 to 10.06
° normal distribution	two-tailed paired t-test	37.01 to 147.8
<sup>p</sup> normal distribution	two-tailed paired t-test	-0.21 to 0.13
<sup>q</sup> normal distribution <sup>r</sup> normal distribution	two-tailed paired t-test one-way ANOVA	1.22 to 110.4 High EGTA 99.09 to 210.7; GDP-β-S 115.9 to 153.4

272

273

### 274 DISCUSSION

- 275 Most reports describing synaptic plasticity in the VTA used electrical stimulation, which can miss
- the possibility of circuit-specificity that can now be probed using optogenetic tools. For example,

LTP<sub>GABA</sub> (Nugent et al., 2007) was found to vary depending on presynaptic source (Simmons et
 al., 2017, Polter et al., 2018). Here we report that inhibitory synapses in the VTA have different
 requirements for inducing LTP depending on the placement of the stimulating electrode.

280

### 281 Synaptic plasticity induction

Using the same stimulation protocol but with the electrode at a site that deviated from the usual 282 placement, we serendipitously discovered that we could induce NMDAR-independent LTP using 283 either HFS or LFS. Pairing postsynaptic cell depolarization with afferent stimulation, to 284 substitute for a strong tetanus, is a classic approach used to induce LTP in the hippocampus 285 286 (Nicoll, 2017). However, this method for inducing LTP is generally due to NMDAR activation. Instead, robust caudal LFS-induced LTP in the VTA was elicited in the presence of an NMDAR 287 antagonist. Previously described LFS-LTD in the VTA is also NMDAR-independent (Dacher and 288 289 Nugent, 2011). How might the same pattern of afferent stimulation result in opposite synaptic plasticity outcomes? One likely explanation is that different electrode locations preferentially 290 291 activate different subsets of afferents in the VTA slice. The VTA dopamine cells are innervated 292 both by local GABA neurons and by GABA projections originating in regions throughout the brain that may differ in protein expression leading to different forms of synaptic plasticity. 293 294 Another possibility is that the timing of inputs differs when using the two stimulating electrode 295 locations; however, we did not observe a significant difference in onset delay, rise slope, or time of peak amplitude of IPSCs from caudal vs. rostral. We speculate that LFS with mild 296 297 depolarization may lead to release of a signaling molecule from the post- or pre-synaptic cell. If different synapses express different receptor subtypes for that signaling molecule, then release 298 via LFS could result in distinct synaptic strength changes. Future experiments will be needed to 299 300 determine if HFS-LTP and LFS-LTP result e.g. from activation by metabotropic glutamate, 301 endocannabinoid, or dopamine receptors.

302

### 303 Low frequency stimulation and synaptic plasticity

304 Numerous studies have shown that LFS induces LTD, often when paired with modest 305 postsynaptic depolarization (Bear and Malenka, 1994, Gutlerner et al., 2002). There are fewer 306 instances where LFS induces LTP, and these generally required pairing with strong depolarization to activate NMDA receptors (Bonci and Malenka, 1999, Ikeda et al., 2007, 307 308 Dringenberg et al., 2014, Lante et al., 2006). Here we found that LFS potentiates VTA GABA 309 synapses with mild depolarization and LFS that did not require NMDAR activation, an apparently rare mechanism at CNS synapses. One other example is at the excitatory synapse 310 from lateral perforant path to dentate gyrus cells, where LFS also potentiates synapses 311 312 independently of NMDAR activation (Gonzalez et al., 2014). However, to our knowledge, ours is the first report of LTP elicited by LFS at GABAergic synapses. 313

314

### 315 GABAergic afferents innervating the VTA

316 Exposure to drugs of abuse causes long-term potentiation (LTP) at excitatory synapses on VTA DA cells (Ungless et al., 2001, Saal et al., 2003). Many drugs of abuse also block LTP<sub>GABA</sub> in the 317 318 VTA (Nugent et al., 2007, Guan and Ye, 2010, Niehaus et al., 2010, Graziane et al., 2013). The net result of these drug-induced changes in synaptic strength is thought to be increased 319 dopamine cell firing via enhanced excitatory drive and disinhibition. However, if more types of 320 321 synaptic plasticity exist than previously suspected, differential effects of drugs of abuse on VTA 322 afferents may produce a more nuanced effect on dopamine cell firing. LTPGABA is expressed at VTA<sub>GABA</sub> $\rightarrow$ VTA but not at RMTg<sub>GABA</sub> $\rightarrow$ VTA synapses; by analogy, it is likely that the HFS- and 323 324 LFS- induced LTP we report here are expressed only at a subset of inputs. It is difficult to be 325 certain precisely which afferents are sufficiently close to the caudal stimulation site to be

activated by our stimulus protocol. Regions other than the RMTg that are located caudal to the VTA with reported GABAergic innervation include: the dorsal raphe, periaqueductal gray, pedunculopontine nucleus, and laterodorsal tegmentum (Beier et al., 2015, Faget et al., 2016, Omelchenko and Sesack, 2010, Ntamati et al., 2018). Given the placement of the caudal electrode in our experiments, it is possible that the presynaptic source of those inputs is from one of these caudal brain regions, although it is alternatively possible that regions located elsewhere in the brain send projections that pass through the caudal stimulation location.

333

In conclusion, depending upon stimulation site, HFS and LFS can induce LTP at GABAergic synapses in the VTA via a mechanism that does not require NMDAR activation. These results support the recent findings that some forms of plasticity, like LTP<sub>GABA</sub> (Simmons et al., 2017, Polter et al., 2018), are selectively expressed at some synapses but not others. Together, this points towards a specificity of synaptic plasticity based upon presynaptic partner and postsynaptic cell identity. Furthermore, this study highlights the fact that there may be plasticity mechanisms in the VTA still to be identified.

- BEAR, M. F. & MALENKA, R. C. 1994. Synaptic plasticity: LTP and LTD. *Curr Opin Neurobiol*,
  4, 389-99.
- BEIER, K. T., STEINBERG, E. E., DELOACH, K. E., XIE, S., MIYAMICHI, K., SCHWARZ, L.,
  GAO, X. J., KREMER, E. J., MALENKA, R. C. & LUO, L. 2015. Circuit Architecture of
  VTA Dopamine Neurons Revealed by Systematic Input-Output Mapping. *Cell*, 162, 622634.
- BONCI, A. & MALENKA, R. C. 1999. Properties and plasticity of excitatory synapses on
   dopaminergic and GABAergic cells in the ventral tegmental area. *The Journal of neuroscience : the official journal of the Society for Neuroscience,* 19, 3723-30.
- BONCI, A. & WILLIAMS, J. T. 1996. A common mechanism mediates long-term changes in
   synaptic transmission after chronic cocaine and morphine. *Neuron*, 16, 631-9.
- BONCI, A. & WILLIAMS, J. T. 1997. Increased probability of GABA release during withdrawal
   from morphine. *J Neurosci*, 17, 796-803.
- BRIGGS, C. A., MCAFEE, D. A. & MCCAMAN, R. E. 1988. Long-term regulation of synaptic
  acetylcholine release and nicotinic transmission: the role of cyclic AMP. *Br J Pharmacol*,
  93, 399-411.
- 358 CAMERON, D. L. & WILLIAMS, J. T. 1993. Dopamine D1 receptors facilitate transmitter 359 release. *Nature*, 366, 344-7.
- CASTRO-ALAMANCOS, M. A. & CALCAGNOTTO, M. E. 1999. Presynaptic long-term
   potentiation in corticothalamic synapses. *J Neurosci*, 19, 9090-7.
- 362 CHAVEZ-NORIEGA, L. E. & STEVENS, C. F. 1994. Increased transmitter release at excitatory
   363 synapses produced by direct activation of adenylate cyclase in rat hippocampal slices. *J* 364 *Neurosci*, 14, 310-7.

DACHER, M. & NUGENT, F. S. 2011. Morphine-induced modulation of LTD at GABAergic
 synapses in the ventral tegmental area. *Neuropharmacology*, 61, 1166-1171.

DRINGENBERG, H. C., BRANFIELD DAY, L. R. & CHOI, D. H. 2014. Chronic fluoxetine
 treatment suppresses plasticity (long-term potentiation) in the mature rodent primary
 auditory cortex in vivo. *Neural Plast*, 2014, 571285.

FAGET, L., OSAKADA, F., DUAN, J., RESSLER, R., JOHNSON, A. B., PROUDFOOT, J. A.,
YOO, J. H., CALLAWAY, E. M. & HNASKO, T. S. 2016. Afferent Inputs to
Neurotransmitter-Defined Cell Types in the Ventral Tegmental Area. *Cell Reports*, 15,
2796-2808.

GONZALEZ, J., MORALES, I. S., VILLARREAL, D. M. & DERRICK, B. E. 2014. Low-frequency
 stimulation induces long-term depression and slow onset long-term potentiation at
 perforant path-dentate gyrus synapses in vivo. *J Neurophysiol*, 111, 1259-73.

377 GRAZIANE, N. M., POLTER, A. M., BRIAND, L. A., PIERCE, R. C. & KAUER, J. A. 2013.
378 Kappa opioid receptors regulate stress-induced cocaine seeking and synaptic plasticity.
379 *Neuron*, 77, 942-954.

GREENGARD, P., JEN, J., NAIRN, A. C. & STEVENS, C. F. 1991. Enhancement of the
 glutamate response by cAMP-dependent protein kinase in hippocampal neurons.
 *Science*, 253, 1135-8.

GUAN, Y.-Z. & YE, J.-H. 2010. Ethanol blocks long-term potentiation of GABAergic synapses in
 the ventral tegmental area involving mu-opioid receptors. *Neuropsychopharmacology :* official publication of the American College of Neuropsychopharmacology, 35, 1841 1849.

GUTLERNER, J. L., PENICK, E. C., SNYDER, E. M. & KAUER, J. A. 2002. Novel protein
 kinase A-dependent long-term depression of excitatory synapses. *Neuron*, 36, 921-31.

HUANG, Y. Y. & KANDEL, E. R. 1994. Recruitment of long-lasting and protein kinase A dependent long-term potentiation in the CA1 region of hippocampus requires repeated
 tetanization. *Learn Mem*, 1, 74-82.

## HUANG, Y. Y. & KANDEL, E. R. 1998. Postsynaptic induction and PKA-dependent expression of LTP in the lateral amygdala. *Neuron*, 21, 169-78.

IKEDA, R., TAKAHASHI, Y., INOUE, K. & KATO, F. 2007. NMDA receptor-independent
 synaptic plasticity in the central amygdala in the rat model of neuropathic pain. *Pain*,
 127, 161-72.

# KODANGATTIL, J. N., DACHER, M., AUTHEMENT, M. E. & NUGENT, F. S. 2013. Spike timing-dependent plasticity at GABAergic synapses in the ventral tegmental area. J *Physiol*, 591, 4699-710.

- 400 LANTE, F., CAVALIER, M., COHEN-SOLAL, C., GUIRAMAND, J. & VIGNES, M. 2006.
  401 Developmental switch from LTD to LTP in low frequency-induced plasticity.
  402 *Hippocampus*, 16, 981-9.
- LINDEN, D. J. & AHN, S. 1999. Activation of presynaptic cAMP-dependent protein kinase is required for induction of cerebellar long-term potentiation. *J Neurosci*, 19, 10221-7.
- LIU, Q.-S., PU, L. & POO, M.-M. 2005. Repeated cocaine exposure in vivo facilitates LTP
  induction in midbrain dopamine neurons. *Nature*, 437, 1027-1031.
- 407 MELIS, M., CAMARINI, R., UNGLESS, M. A. & BONCI, A. 2002. Long-lasting potentiation of
   408 GABAergic synapses in dopamine neurons after a single in vivo ethanol exposure. J
   409 *Neurosci*, 22, 2074-2082.
- MELLOR, J., NICOLL, R. A. & SCHMITZ, D. 2002. Mediation of hippocampal mossy fiber long term potentiation by presynaptic lh channels. *Science*, 295, 143-7.
- 412 NICOLL, R. A. 2017. Review A Brief History of Long-Term Potentiation. Neuron, 93, 281-290.

413

inhibitory synapses in the ventral tegmental area. European Journal of Neuroscience, 414 32, 108-117. 415 NTAMATI, N. R., CREED, M., ACHARGUI, R. & LUSCHER, C. 2018. Periaqueductal efferents 416 to dopamine and GABA neurons of the VTA. PLoS One, 13, e0190297. 417 NUGENT, F. S., NIEHAUS, J. L. & KAUER, J. A. 2009. PKG and PKA Signaling in LTP at 418 GABAergic Synapses. Neuropsychopharmacology, 345, 1829-1842. 419 420 NUGENT, F. S., PENICK, E. C. & KAUER, J. A. 2007. Opioids block long-term potentiation of inhibitory synapses. Nature, 446, 1086-1090. 421 OMELCHENKO, N. & SESACK, S. R. 2010. Periagueductal gray afferents synapse onto 422 dopamine and GABA neurons in the rat ventral tegmental area. J Neurosci Res, 88, 981-423 91. 424 PADGETT, C. L., LALIVE, A. L., TAN, K. R., TERUNUMA, M., MUNOZ, M. B., PANGALOS, M. 425 N., MART??NEZ-HERN??NDEZ, J., WATANABE, M., MOSS, S. J., LUJ??N, R., 426 427 L??SCHER, C. & SLESINGER, P. A. 2012. Methamphetamine-Evoked Depression of GABA B Receptor Signaling in GABA Neurons of the VTA. Neuron, 73, 978-989. 428 POLTER, A. M., BARCOMB, K., TSUDA, A. C. & KAUER, J. A. 2018. Synaptic function and 429 430 plasticity in identified inhibitory inputs onto VTA dopamine neurons. Eur J Neurosci, 47, 1208-1218. 431 POLTER, A. M., BISHOP, R. A., BRIAND, L. A., GRAZIANE, N. M., PIERCE, R. C. & KAUER, 432 433 J. A. 2014. Poststress block of kappa opioid receptors rescues long-term potentiation of inhibitory synapses and prevents reinstatement of cocaine seeking. Biological 434

NIEHAUS, J. L., MURALI, M. & KAUER, J. A. 2010. Drugs of abuse and stress impair LTP at

435 *Psychiatry*, 76, 785-793.

SAAL, D., DONG, Y., BONCI, A. & MALENKA, R. C. 2003. Drugs of abuse and stress trigger a
common synaptic adaptation in dopamine neurons. *Neuron*, 37, 577-582.

SALIN, P. A., MALENKA, R. C. & NICOLL, R. A. 1996. Cyclic AMP mediates a presynaptic form
of LTP at cerebellar parallel fiber synapses. *Neuron*, 16, 797-803.

SIMMONS, D. V., PETKO, A. K. & PALADINI, C. A. 2017. Differential expression of long-term
potentiation among identified inhibitory inputs to dopamine neurons. *J Neurophysiol,*118, 1998-2008.

TING, J. T., DAIGLE, T. L., CHEN, Q. & FENG, G. 2014. Acute brain slice methods for adult
and aging animals: application of targeted patch clamp analysis and optogenetics. *Methods Mol Biol*, 1183, 221-42.

UNGLESS, M. A., WHISTLER, J. L., MALENKA, R. C. & BONCI, A. 2001. Single cocaine
exposure in vivo induces long-term potentiation in dopamine neurons. *Nature*, 411, 5837.

WATABE-UCHIDA, M., ZHU, L., OGAWA, S. K., VAMANRAO, A. & UCHIDA, N. 2012. WholeBrain Mapping of Direct Inputs to Midbrain Dopamine Neurons. *Neuron*, 74, 858-873.

451 WEISSKOPF, M. G., CASTILLO, P. E., ZALUTSKY, R. A. & NICOLL, R. A. 1994. Mediation of 452 hippocampal mossy fiber long-term potentiation by cyclic AMP. *Science*, 265, 1878-82.

ZHAO, S., TING, J. T., ATALLAH, H. E., QIU, L., TAN, J., GLOSS, B., AUGUSTINE, G. J.,
DEISSEROTH, K., LUO, M., GRAYBIEL, A. M. & FENG, G. 2011. Cell type-specific
channelrhodopsin-2 transgenic mice for optogenetic dissection of neural circuitry
function. *Nat Methods*, 8, 745-52.

ZHUANG, X., MASSON, J., GINGRICH, J. A., RAYPORT, S. & HEN, R. 2005. Targeted gene
expression in dopamine and serotonin neurons of the mouse brain. *J Neurosci Methods*,
143, 27-32.

460

### 461 FIGURES & LEGENDS

### 462 Figure 1. Electrical stimulation in horizontal midbrain slices

A. Recording setup illustrating caudal or rostral placements of the bipolar stimulating electrodes.
Analysis of caudal vs. rostral IPSC: B. onset delay, C. rise slope, and D. time to peak amplitude.
E. Example IPSCs illustrating control IPSCs (black) and in the μ-opioid receptor agonist,
DAMGO (1 μM)(green), for caudal or rostral inputs, and F. Mean IPSC amplitude depression
after DAMGO (1 μM), for each input.

468 Error bars represent S.E.M.

469

### 470 Figure 2. Location of electrical stimulation determines expression of synaptic plasticity

A. Representative experiment showing LTP induction by HFS with a caudal electrode 471 472 placement. Inset: baseline (black traces) and 10-20 min after HFS (red traces). B. Mean IPSC 473 amplitudes from a 10 min baseline and 10-20 min after caudal HFS (n = 16 cells). In this and 474 subsequent figures, thicker black symbols/lines represent the mean response across all cells. C. Representative experiment with HFS of a rostral electrode. Inset: baseline (black traces) and 475 10-20 min after HFS (red traces). D. Mean IPSC amplitudes from a 10 min baseline to 10-20 476 min after rostral HFS (n = 6 cells). E. Time course of averaged IPSC amplitudes before and 477 after HFS. (closed symbols = caudal, open symbols = rostral) F. Paired pulse ratios before and 478 479 after caudal HFS from each cell that potentiated >10% of basal values (n = 12 cells). G.  $1/CV^2$ 480 values before and after caudal HFS from each cell that potentiated >10% of basal values (n = 481 12 cells).

482 \*p < .05, paired t-test of amplitude of 10 min baseline vs.10-20 min after HFS.

483 Error bars represent S.E.M.

### 486 Figure 3. Low frequency stimulation of caudal electrode induces LTP

A. Representative experiment with LFS with a caudal electrode placement without APV, or B.
with APV. Insets: baseline (black traces) and 10-20 min after LFS (red traces). C. Time course
of averaged IPSC amplitudes before and after LFS. D. Mean IPSC amplitudes from a 10 min
baseline to 10-20 min after caudal LFS (n = 38 cells). E. Paired pulse ratios before and after
caudal LFS from each cell that potentiated >10% of basal values (n = 22 cells). F. 1/CV<sup>2</sup> values
before and after caudal LFS from each cell that potentiated >10% of basal values (n = 19 cells).
D., E., F. Grey symbols/lines no APV, black symbols/lines, with APV present.

494 \*p < .05, paired t-test of amplitude of 10 min baseline vs.10-20 min after LFS.

495 Error bars represent S.E.M.

496

485

### 497 Figure 4. No effect with low frequency optical stimulation of VGAT<sup>+</sup> synapses

A. Representative experiment with optical LFS. Inset: baseline (black traces) and 10-20 min
after LFS (red traces). B. Time course of averaged IPSC amplitudes before and after LFS. C.

500 Mean IPSC amplitudes from a 10 min baseline to 10-20 min after optical LFS (n = 7 cells).

501 Error bars represent S.E.M.

502

# Figure 5. Forskolin potentiates GABAergic synapses evoked with caudal stimulation but does not prevent subsequent potentiation by caudal LFS

**A.** Representative experiment with 10  $\mu$ M forskolin. Inset: baseline (black traces) and in forskolin (gray traces). **B.** Time course of averaged IPSC amplitudes before and during forskolin. **C.** Mean IPSC amplitudes from a 10 min baseline to 10-20 min after forskolin addition (n = 14 cells). **D.** Representative experiment with caudal LFS after potentiation by 10  $\mu$ M forskolin. Inset: baseline in forskolin (gray traces) and 10-20 min after LFS (red traces). **E.** Time course of averaged IPSC amplitudes before and after caudal LFS after forskolin-induced potentiation was established`1. **F.** Mean IPSC amplitudes from a 10 min baseline to 10-20 min after forskolin (n = 10 cells).

p < .05, paired t-test of amplitude of 10 min baseline vs.10-20 min after forskolin or LFS.

514 Error bars represent S.E.M.

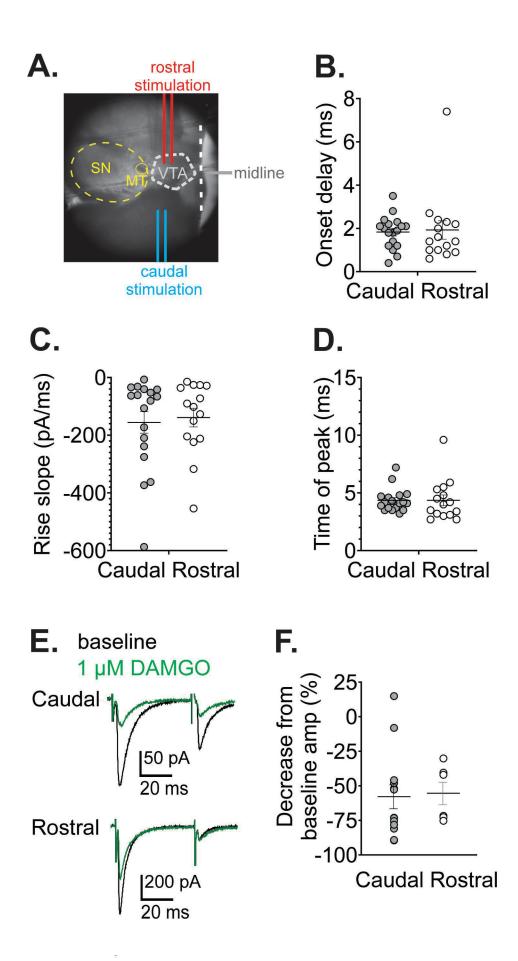
515

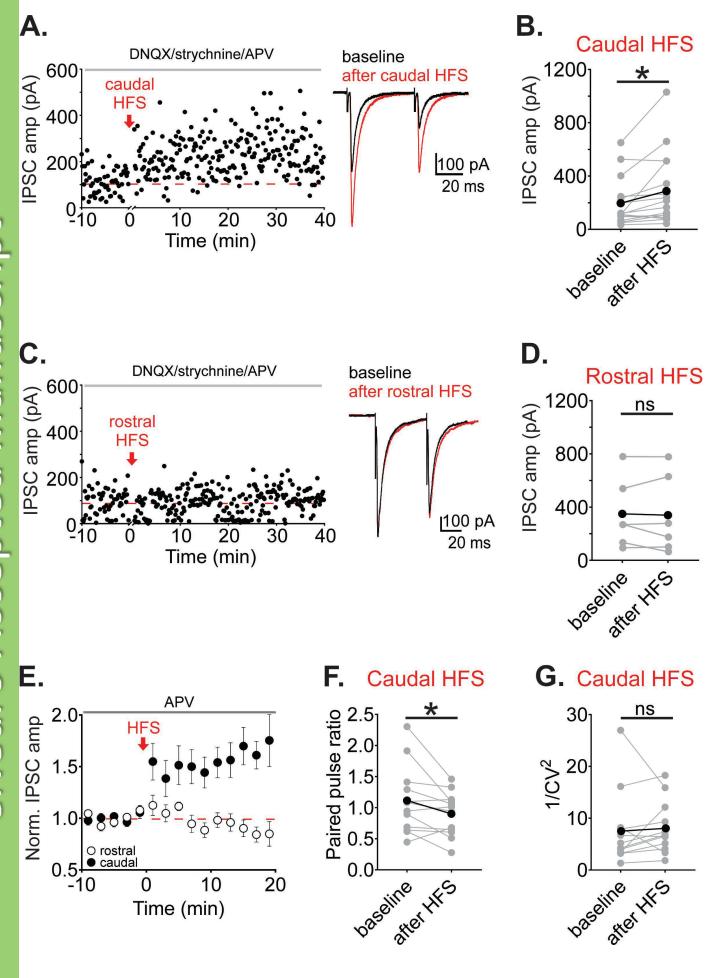
### 516 Figure 6. LFS-induced LTP does not require postsynaptic calcium elevation or GPCR 517 activation

518 A. Representative experiment with caudal LFS when 15 mM EGTA was included in the patch 519 pipette. Inset: baseline (black traces) and 10-20 min after LFS (red traces). B. Time course of 520 averaged IPSC amplitudes before and after caudal LFS with 15 mM EGTA. C. Mean IPSC amplitudes from a 10 min baseline to 10-20 min after caudal LFS with 15 mM EGTA (n = 8 521 cells). D. Representative experiment with caudal LFS when 1 mM GDP-β-S was included in the 522 patch pipette intracellular solution. Inset: baseline (black traces) and 10-20 min after LFS (red 523 traces). E. Time course of averaged IPSC amplitudes before and after caudal LFS with 1 mM 524 GDP-β-S. F. Mean IPSC amplitudes from a 10 min baseline to 10-20 min after LFS with 1 mM 525 GDP- $\beta$ -S (n = 8 cells). 526

p < .05, paired t-test of amplitude of 10 min baseline vs.10-20 min after LFS.

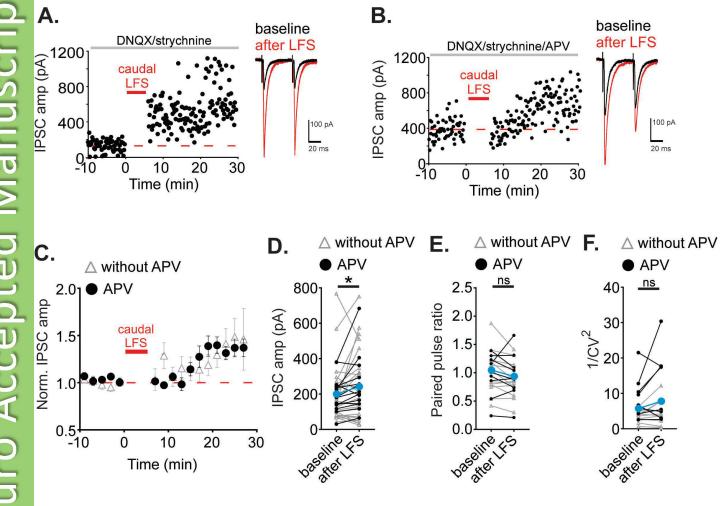
528 Error bars represent S.E.M.



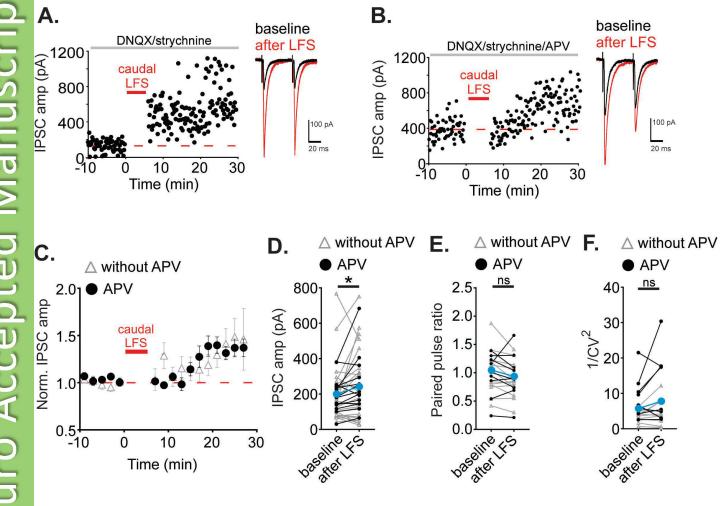


eNeuro Accepted Manuscript









<u>eNeuro Accepted Manuscript</u>

